BIOCHEMISTRY
including biophysical chemistry & molecular biology

Article

pubs.acs.org/biochemistry

Novel Interactions of the TRTK12 Peptide with S100 Protein Family Members: Specificity and Thermodynamic Characterization

Lucas N. Wafer,[†] Franco O. Tzul,[†] Pranav P. Pandharipande,[‡] and George I. Makhatadze*,[†]

[†]Department of Biology and [‡]Department of Chemical and Biological Engineering, Center for Biotechnology and Interdisciplinary Studies, Rensselaer Polytechnic Institute, Troy, New York 12180, United States

Supporting Information

ABSTRACT: The S100 protein family consists of small, dimeric proteins that exert their biological functions in response to changing calcium concentrations. S100B is the best-studied member and has been shown to interact with more than 20 binding partners in a calcium-dependent manner. The TRTK12 peptide, derived from the consensus binding sequence for S100B, has previously been found to interact with S100A1 and has been proposed to be a general binding partner of the S100 family. To test this hypothesis and gain a better understanding of the specificity of binding for the S100 proteins, 16 members of the human S100 family were screened against this peptide and its alanine variants. Novel interactions were found with only two family members, S100P and S100A2, indicating that TRTK12 selectively interacts with a small subset of the S100 proteins. Substantial promiscuity was observed in the binding site of S100B thereby accommodating variations in the peptide sequence, while S100A1, S100A2, and S100P exhibited larger differences in the binding constants for the TRTK12 alanine variants. This suggests that single-point substitutions can be used to selectively modulate the affinity of TRTK12 peptides for individual S100 proteins. This study has important implications for the rational drug design of inhibitors for the S100 proteins, which are involved in a variety of cancers and neurodegenerative diseases.

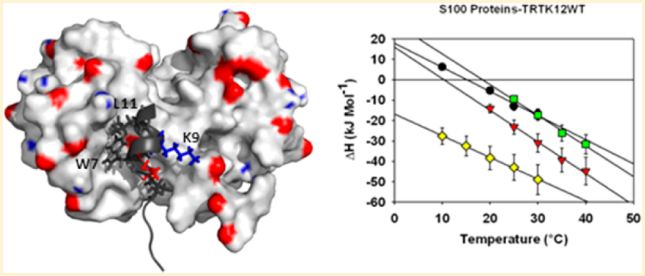

The S100 protein family consists of approximately 25 members found exclusively in vertebrates, making it the largest subset of the EF-hand, calcium-binding proteins.[1] The name derives from the fact that many members are soluble in 100% ammonium sulfate at neutral pH.[2] These proteins are expressed in a tissue-specific manner and have been implicated in a variety of intracellular and extracellular functions, including cell growth and differentiation, cytoskeleton dynamics, regulation of calcium homeostasis, inflammation response, and protein phosphorylation.[1,3−6] In addition, the expression levels of the S100 proteins have been directly correlated to the severity of neurodegenerative disorders,[7−11] inflammatory diseases such as irritable bowel syndrome,[12−15] cardiomyopathies,[16,17] and various cancers.[6,18−24]

S100 proteins are relatively small (9−13 kDa) and exist almost exclusively as homo- or heterodimers in solution.[25] Each S100 protein monomer consists of four α-helices, with helices I and IV arranged in an antiparallel orientation.[1,26] Calcium binding induces a significant structural rearrangement in the S100 proteins that has been well-documented by X-ray crystallography and solution nuclear magnetic resonance (NMR) spectroscopy.[27−32] During this conformational change, helix III reorients itself (>40°) relative to helices II and IV to expose a hydrophobic binding pocket that allows interactions with target proteins and peptides.[27] Because the S100 proteins appeared to be functionally distinct from related, calcium-binding proteins, such as calmodulin and parvalbumin, early work focused on identifying high-affinity biological targets to improve our understanding of the molecular basis of recognition.[33−38]

In 1995, Ivankenov et al. screened a phage display library against S100B and provided the first consensus binding sequence for the S100 proteins [(K/R)-(L/I)-X-W-X-X-I-L].[35] A search of the available protein sequences showed a highly homologous region in the C-terminus of the actin-binding protein CapZ (T-R-T-K-I-D-W-N-K-I-L-S).[35] This sequence was later termed TRTK12.[35] Subsequent studies have shown that this peptide interacts with the two C-terminal helices of S100B (Figure 1), as well as the hinge region, and was able to compete with binding for other known targets.[35,39−46] Furthermore, it was shown to bind S100A1, leading some to propose that TRTK12 represents a general binding motif for the S100 protein family.[32]

To gain a better understanding of the specificity of binding within the S100 protein family, we screened the proposed consensus binding sequence (TRTK12) against representative members of the human S100 protein family, using isothermal titration calorimetry (ITC) and steady-state emission fluorescence. Unexpectedly, TRTK12 was found to selectively interact with a small subset of S100 proteins. We confirmed previously reported interactions with S100B and S100A1. In

Received: June 18, 2013
Revised: July 30, 2013
Published: July 30, 2013

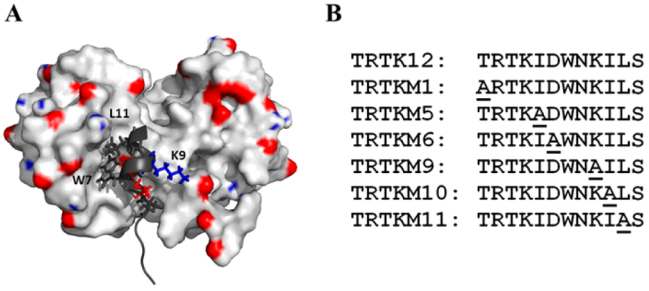

Figure 1. (A) NMR solution structure of the wild-type TRTK12 peptide with rat S100B (PDB entry 1MWN).[40] For the sake of clarity, the binding pocket of a single S100B monomer is shown. Key residues from the TRTK12 peptide are colored and labeled. (B) List of TRTK12 peptide sequences. Alanine-substitued residues are underlined.

addition, novel interactions of the wild-type peptide were detected with S100A2 and S100P. These interactions were characterized in detail using ITC and stopped-flow spectroscopy. The subset of S100 proteins that bound to wild-type TRTK12 was also screened against a variety of TRTK12 alanine variants. Both the thermodynamics and kinetics of binding were then characterized to ascertain the individual binding contribution of amino acids within the TRTK12 peptide sequence. For the variants, alanine substitutions were chosen according to the residue-specific interactions in the available structures of the bound S100−TRTK12 complexes (Figure 1).[32,43,44] The TRTKM6 (Asp6Ala) and TRTKM9 (Lys9Ala) variants were selected to probe the electrostatic interactions because ionic strength has been reported to significantly affect the binding affinity of the TRTK12 peptide, albeit in a contradictory manner.[42,47] The TRTKM5 (Ile5Ala), TRTKM10 (Ile10Ala), and TRTKM11 (Leu11Ala) variants were selected to query the effects of the hydrophobic residues because the available structures of the S100−TRTK12 complexes suggest that the leucine and isoleucine residues from the peptide contribute most of the buried surface area in the complex with S100B and S100A1.[29,44] The TRTKM1 (Thr1Ala) variant was used as a control for the N-terminal residues, which have been observed to be unstructured and solvent-exposed in the bound complex.[32,40,43,44] The TRTK12 peptide variants were found to have unique binding affinities, changes in heat capacity upon binding, and dissociation rate constants for individual S100 proteins. These dissimilarities suggest that alanine variants of TRTK12 can be used as a starting point for potential peptide-based inhibitors of particular subsets of the S100 proteins.

EXPERIMENTAL PROCEDURES

Protein/Peptide Purification. Representative members of the S100 protein family, including human S100A1, S100A2, S100A3, S100A4, S100A5, S100A6, S100A7, S100A8, S100A9, S100A10, S100A11, S100A12, S100A13, S100P, S100Z, and S100B, were overexpressed in *Escherichia coli* and purified as previously described.[48−51] The protein concentrations were determined using molar extinction coefficients at 280 nm (ε_{280}) of 1490 M^{-1} cm^{-1} for S100B, 2980 M^{-1} cm^{-1} for S100P, 2980 M^{-1} cm^{-1} for S100Z, 8480 M^{-1} cm^{-1} for S100A1, 2980 M^{-1} cm^{-1} for S100A2, 14440 M^{-1} cm^{-1} for S100A3, 2980 M^{-1} cm^{-1} for S100A4, 4470 M^{-1} cm^{-1} for S100A5, 4470 M^{-1} cm^{-1} for S100A6, 4470 M^{-1} cm^{-1} for S100A7, 11460 M^{-1} cm^{-1} for S100A8, 6990 M^{-1} cm^{-1} for S100A9, 2980 M^{-1} cm^{-1} for S100A10, 4470 M^{-1} cm^{-1} for S100A11, 2980 M^{-1} cm^{-1} for S100A12, and 6990 M^{-1} cm^{-1} for S100A13.

All peptides were synthesized at the Pennsylvania State College of Medicine Macromolecular Core Facility using standard Fmoc chemistry. The N- and C-termini were acetylated and amidated, respectively. The TRTK12 wild-type peptide (Ac-TRTKIDWNKILS-NH_2) is derived from the actin-binding protein CapZ and has previously been used in structural studies.[3,5−7] The alanine-substituted variants of this sequence, namely TRTKM1 (Ac-ARTKIDWNKILS-NH_2), TRTKM5 (Ac-TRTKADWNKILS-NH_2), TRTKM6 (Ac-TRTKIAWNKILS-NH_2), TRTKM9 (Ac-TRTKIDWNAILS-NH_2), TRTKM10 (Ac-TRTKIDWNKALS-NH_2), and TRTKM11 (Ac-TRTKIDWNKIAS-NH_2), were prepared in a similar manner as the wild type. The peptides were purified using a C18 reverse phase column using a 0 to 100% methanol gradient in the presence of 0.05−0.065% trifluoroacetic acid,[50,51] and their masses were confirmed via matrix-assisted laser desorption ionization time-of-flight mass spectrometry (MALDI-TOF-MS) on a Bruker UltraFlex III instrument. The concentration of all peptides was determined using a molar extinction coefficient of 5500 M^{-1} cm^{-1} at 280 nm (ε_{280}) for TRTK12.[52]

Isothermal Titration Calorimetry. ITC measurements were performed using a VP-ITC instrument (MicroCal, Inc., Northhampton, MA) as previously described.[50,51,53,54] Prior to all experiments, the protein and peptide were extensively dialyzed into a binding buffer containing 20 mM Tris base, 0.2 mM disodium EDTA, 1 mM TCEP, and 5 mM calcium chloride (pH 7.5). Additional experiments were performed in the same buffer but with 5 mM EDTA instead of 5 mM calcium chloride to test the calcium-dependence of binding. In general, 0.5−4 mM peptide was injected in 4−10 μL increments into the sample cell (1.5 mL) containing 20−200 μM protein. Because of the low solubility of the TRTKM9 peptide, all titrations performed with this peptide were performed with the protein solution in the syringe and the peptide in the cell. Experiments were performed between 5 and 40 °C, in 5 °C increments. In cases where the enthalpy of binding, ΔH, was close to zero and thus no heat effect was observed, the titration was stopped after three injections. The heat of dilution was measured prior to each experiment by injecting the peptide into buffer at least four times and in all cases was found to be negligible relative to the protein/peptide solution heats. The resulting binding isotherms were analyzed using the Origin scripts for ITC data analysis provided by MicroCal, Inc. The following models were analyzed, in order of increasing complexity, and the simplest model that accurately fit the data was accepted.

Single-set of identical binding sites model, with one or two peptides per S100 dimer:[50,55]

$$Q = \frac{n[\text{cell}]_t \Delta H_{cal} V_o}{2}\left(A - \sqrt{A^2 - \frac{4[\text{syringe}]_t}{n[\text{cell}]_t}}\right) \quad (1)$$

where Q is the integral heat at each injection, $A = 1 + [\text{syringe}]_t/(n[\text{cell}]_t) + [\text{syringe}]_t/[n(1/K_d)[\text{cell}]_t]$, n is the stoichiometry of the protein−peptide complex, ΔH_{cal} is the molar heat of peptide binding, V_o is the active cell volume, $[\text{syringe}]_t$ is the total concentration of the peptide/protein solution in the ITC syringe, $[\text{cell}]_t$ is the total concentration of the protein/peptide solution in the ITC cell, and K_a is the association constant.

dx.doi.org/10.1021/bi400788s | *Biochemistry* 2013, 52, 5844−5856

Two-sequential binding sites model, with two peptides per S100 dimer:[50,55]

$$Q = [\text{cell}]_t V_o\{[\Delta H_{cal1}(1/K_{d1})[\text{syringe}]_t + (\Delta H_{cal1} + \Delta H_{cal2})(1/K_{d1})(1/K_{d2})[\text{syringe}]_t^2] / [1 + [\text{syringe}]_t(1/K_{d1}) + 1 + (1/K_{d1})(1/K_{d2})[\text{syringe}]_t^2]\} \quad (2)$$

where Q is the integral heat at each injection, ΔH_{cal1} and ΔH_{cal2} are the molar heats of peptide binding, V_o is the active cell volume, K_{d1} and K_{d2} are the dissociation constants for binding to sites 1 and 2, respectively, and ΔH_{cal1} and ΔH_{cal2} are the calorimetric enthalpies for binding to sites 1 and 2, respectively.

Fluorescence Spectroscopy. Steady-state fluorescence titrations were performed using a Fluoromax-4 spectrofluorometer (Horiba Jobin Yvon, Kyoto, Japan) operating FluorEssence version 3.5. A cuvette with a 3 mm excitation path length was used throughout all experiments. All TRTK12 peptides contain a Trp residue. In the available structures of the S100 proteins in complex with the wild-type peptide (S100B and S100A1), this tryptophan becomes buried in a hydrophobic region upon binding. Therefore, changes in Trp emission fluorescence intensity were used to monitor interactions between the TRTK12 peptides and S100 proteins. The experiments were performed in binding buffer at 25 ± 0.2 °C using a thermostated cell holder. The solution was excited at 295 nm and the emission spectra were monitored from 305 to 420 nm to monitor changes in λ_{max}; a wavelength of 350 nm was used to specifically monitor changes in intensity. The initial concentration of the TRTK12 peptides in the fluorescence cell was 2−8 μM. Small aliquots of the concentrated protein were added until signal saturation was reached or until the fluorescence signal deviated from unity due to inner filter effects. The experimental emission spectra were corrected by subtracting the emission control spectra of protein added to buffer in the absence of peptide. The fluorescence intensity was also corrected for fluctuations in lamp intensity by dividing the fluorescence signal by the lamp intensity. The data were fit to a single-site binding model using the Nonlinear Regression Analysis Program (NLREG)[56] and the following equation:

$$Q = \frac{Q_{max}}{2[\text{cell}]_{total}}\left(A - \sqrt{A^2 - n[\text{cell}]_{total}[\text{titrant}]_{total}}\right) \quad (3)$$

where Q equals the fluorescence intensity at each titration step, Q_{max} equals the maximal intensity for the fully saturated peptide, $[\text{cell}]_{total}$ equals the molar concentration of the peptide at each step, $A = K_d + [\text{cell}]_{total} + n[\text{titrant}]_{total}$, n equals the number of binding sites, and $[\text{titrant}]_{total}$ equals the molar concentration of the protein at each step.

Anisotropy titrations were performed in the same manner as described above, but using vertical (V) or horizontal (H) excitation and emission polarizations (I_{VV}, I_{VH}, I_{HH}, and I_{HV}). The G factor was calculated as

$$G = \frac{I_{HV}}{I_{HH}} \quad (4)$$

where I_{HV} and I_{HH} represent the corrected intensities for the horizontally polarized light of the peptide in solution. The anisotropy was calculated as

$$\langle r \rangle = \frac{I_{VV} - GI_{VH}}{I_{VV} + 2GI_{VH}} \quad (5)$$

where $\langle r \rangle$ represents the anisotropy at a given titration step and I_{VV} and I_{VH} represent the corrected intensities of the vertically polarized light.

The relative exposure of the tryptophan residue in the peptide−protein complex was assayed using dynamic quenching with acrylamide. Titrations were performed using 4−8 μM solutions of the peptide in the presence or absence of saturating amounts of the S100 proteins and 5 mM $CaCl_2$ or 5 mM EDTA. In cases where the affinity for the complex was low, the protein concentration was limited by the inner filter effect. Titrations were performed until the final concentration of acrylamide was ∼0.6 M, and the data were then fit to the modified Stern−Volmer equation:[54,57]

$$\frac{I}{I_o} = (1 + K_{SV}[Q])e^{V[Q]} \quad (6)$$

where I_o is the initial fluorescence intensity, I is the intensity at a given titration step, K_{SV} is the Stern−Volmer constant, [Q] is the acrylamide concentration at a given titration step, and V[Q] is the constant describing the static component of the quenching reaction. The intensity was corrected for dilution, and the average values are reported.

Structure-Based Calculations of ΔC_p. Using the available three-dimensional structures of S100A1, S100A2, S100B, and S100P in the calcium-bound state and/or in complex with a peptide target, ΔASA_{tot} was calculated as previously described.[58] In cases where no structure was available, homology models of the peptide-bound state were generated using Modeler[59] and PDB entries 1MQN,[40] 1MQ1,[43] 3IQQ,[44] and 2KBM.[32] Changes in the accessible surface area upon binding, ΔASA_{total}, were calculated as previously described.[50,51,54] Changes in ΔASA were further subdivided into four categories (aliphatic surface area, aromatic surface area, peptide backbone surface area, and polar surface area) and converted into ΔC_p using the following empirical relationship:[50,51,58,60,61]

$$\Delta C_p = 2.14\Delta ASA_{alp} + 1.55\Delta ASA_{arm} - 1.81\Delta ASA_{bb} - 0.88\Delta ASA_{pol} \quad (7)$$

where ΔASA_{alp}, ΔASA_{arm}, and ΔASA_{pol} values are the changes in ASA for aliphatic, aromatic, and polar amino acids, respectively, and ΔASA_{bb} values are the changes in ASA for the polypeptide backbone.

Kinetic Stopped-Flow k_{off} Measurements. Measurements of protein−peptide dissociation rate constants (k_{off}) were performed using standard stopped-flow methods. Data were collected using a JASCO J-815 spectropolarimeter equipped with an SFM 300 mixing module (BioLogic Science Instruments), containing an HDS mixer and a FC-15 observation cuvette. The k_{off} rate constants were evaluated at a minimum of three temperatures between 5 and 35 °C. The temperature of the sample chamber was regulated using a circulating water bath. A mercury lamp source was used for peptide tryptophan excitation at 295 nm. The emission fluorescence was collected using an N-WG 320 cutoff filter (BioLogic Science Instruments). Slit widths were adjusted from 3 to 5 nm to eliminate or minimize photobleaching. Voltages applied to the photomultiplier tube were set accordingly and ranged from 700 to 850 V. Kinetic traces were collected under

dx.doi.org/10.1021/bi400788s | Biochemistry 2013, 52, 5844−5856

an optimal set of push volumes and flow rates for the SFM 300 instrument and kept constant for all experiments. Because peptide binding is calcium-dependent, peptide dissociation was initiated by calcium chelation. For this, preformed protein−peptide complexes (6 or 12 μM peptide) in the binding buffer described above were mixed in a 1:1 mixing ratio with 40 mM EDTA. Special care was taken to control for inner filter effects by limiting the protein:peptide ratio.

Using the Bio-Kine32 software package (BioLogic Science Instruments), rate constants, k_{off}, were obtained by fitting the exponential change of the emission fluorescence intensity from EDTA-induced peptide dissociation to the following equation:

$$I(t) = \mathrm{XT} + y_0 + A\mathrm{e}^{\pm k_{app}T} \quad (8)$$

where $I(t)$ is the fluorescence intensity as a function of time, y_0 is the initial fluorescence intensity, A is the amplitude of the change between the initial and final fluorescence intensity, k_{app} is the observed kinetic rate constant associated with the fluorescence intensity relaxation, and XT is the sloping baseline correction used in the Bio-Kine32 software, which accounts for the photobleaching effect. Errors were calculated from the standard deviation of five independent traces. A dead time of 4.0 ms was electronically estimated with BioLogic's Bio-Kine32 software and experimentally confirmed using the dead-time assessment procedure of Peterman et al.[62] Because the experimentally determined rate constants were sufficiently slow, no dead-time data correction was performed.

RESULTS

The TRTK12 peptide has been shown to bind human S100B and human S100A1 in a calcium-dependent manner[29,32,35,40−44,46,47] and has been proposed to be a general S100 protein-binding motif.[32] To probe the specificity of TRTK12 for these proteins, 16 representative members of the human S100 protein family were screened for binding using isothermal titration calorimetry (ITC) and emission fluorescence. Unexpectedly, novel interactions were detected with only two S100 proteins: S100A2 and S100P. To gain a better understanding of these interactions, the binding of the wild-type peptide and its alanine variants was further characterized using several biophysical methods.

Interactions of TRTK12 Peptides with S100B. Figure 2A shows the binding isotherm obtained from ITC experiments at 25 °C in which the wild-type TRTK12 peptide was titrated into S100B in the presence of 5 mM $CaCl_2$. As reported previously,[4] two peptides interact with the S100B dimer through identical binding sites (eq 1; n = 2). The dissociation constant, K_d, obtained from the fit, 1.7 ± 0.1 μM, is in good agreement with previously reported values.[44,47,50] The binding model is consistent with structures derived from X-ray crystallography and solution NMR involving complexes of TRTK12 and S100B from several orthologs (*Homo sapiens*, *Rattus norveggicus*, and *Bos taurus*).[5,17,18] ITC experiments were performed over the temperature range of 5−40 °C. In addition, the thermodynamics of binding were measured for six alanine variants of TRTK12 (see Experimental Procedures for abbreviated names and sequences). All peptides, with the exception of TRTKM11, bind with a stoichiometry similar to that of the wild type, i.e., two peptides per S100B dimer (eq 1; n = 2). TRTKM11 appears to interact with a different stoichiometry of one peptide per S100B dimer (eq 1; n = 1). This stoichiometry has previously been observed for several peptides binding to the

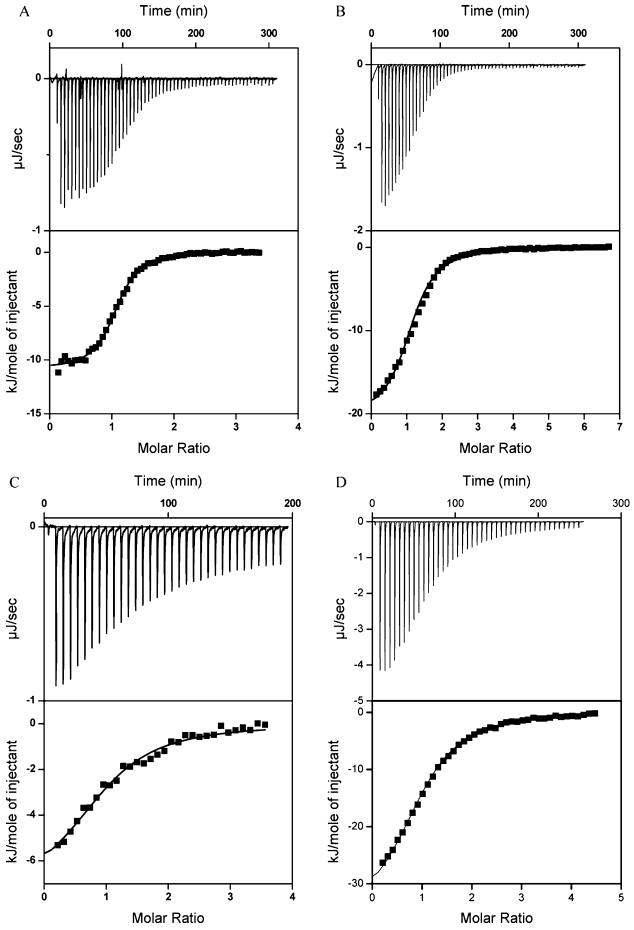

Figure 2. Examples of ITC experiments showing the binding of TRTK12 to S100B, S100A1, S100A2, and S100P in the presence of calcium. The top plots in each panel represent the raw heat effects as a function of time and the bottom plots represent the cumulative heat effects (■) as a function of the molar ratio of peptide to protein and the fits to the experimental data using eq 1 (—) for binding of TRTK12 to S100B at 25 °C (A), binding of TRTK12 to S100A1 at 25 °C (B), binding of TRTK12 to S100A2 at 25 °C (C), and binding of TRTK12 to S100P at 25 °C (D).

S100 proteins.[50,63−69] The dissociation constants of wild type and alanine peptides are listed in Table 1.

Figure 3A shows the temperature dependence of the enthalpy of binding, ΔH_{cal}, of the wild-type peptide and alanine variants to S100B. The slope of the temperature dependence corresponds to the heat capacity change upon binding, ΔC_p, and these values are summarized in Table 1. It has previously been shown that ΔC_p can be predicted using empirical changes in the accessible surface area upon binding, provided that accurate structural models are available.[2,4,14,21] The experimentally determined heat capacity change for the S100B−TRTK12 interaction (−1.2 ± 0.2 kJ mol^{-1} K^{-1}) is in excellent agreement with the structure-based calculated values (Table 1). In addition, the values obtained for all alanine variants but TRTKM11 are within error of the wild-type ΔC_p value, suggesting they interact with S100B through a similar structural mode. This is also expected on the basis of the structure-based calculations of ΔC_p using homology models of the alanine variants (Table 1). Again, the only notable exception is the TRTKM11 variant, which interacts with the S100B dimer with a novel stoichiometry of one peptide per

dx.doi.org/10.1021/bi400788s | *Biochemistry* 2013, 52, 5844−5856

Table 1. Summary of the Dissociation Constants, Changes in Heat Capacity upon Binding, and Kinetic Rate Constants of the TRTK12 Wild-Type Peptide and Alanine Variants Binding to S100B at 25 °C

peptide	K_d[a] (μM)	$\Delta C_{p,exp}$[b] (kJ mol^{-1} K^{-1})	$\Delta C_{p,calc}$[c] (kJ mol^{-1} K^{-1})	k_{off} (s^{-1})[d]	k_{on} ($\times 10^7$ M^{-1} s^{-1})[e]
TRTK12	1.7 ± 0.1 (3 ± 1)	−1.2 ± 0.2	−1.4 ± 0.1	53 ± 4	3.1 ± 0.3
TRTKM1	2.9 ± 1.0 (0.2 ± 0.1)	−1.2 ± 0.1	−1.3 ± 0.1	34 ± 2	1.2 ± 0.1
TRTKM5	1.2 ± 0.4 (0.6 ± 0.6)	−1.0 ± 0.1	−1.2 ± 0.1	66 ± 7	5.5 ± 1.9
TRTKM6	1.3 ± 0.6 (5 ± 1)	−1.3 ± 0.1	−1.5 ± 0.1	31 ± 1	6.6 ± 1.0
TRTKM9	1.7 ± 0.1 (2 ± 1)	−1.5 ± 0.1	−1.5 ± 0.1	53 ± 8	3.1 ± 0.5
TRTKM10	3.4 ± 1.0 (1 ± 0.1)	−1.0 ± 0.1	−1.1 ± 0.1	36 ± 8	1.1 ± 0.4
TRTKM11	3.8 ± 1.0 (10 ± 3)	−1.6 ± 0.2	−1.3 ± 0.1	na[f]	na[f]

[a]Dissociation constants obtained using ITC. Values in parentheses were obtained using emission fluorescence assays. [b]Experimentally determined changes in heat capacity upon binding (Figure 3). [c]Structure-based calculations (see eq 7) using the average value from homology models based on the human S100B dimer binding to two peptides using PDB entries 1MQ1,[43] 1MWN,[40] and 3IQQ.[44] [d]k_{off} values obtained using fluorescence stopped-flow spectroscopy (eq 8). [e]k_{on} values were calculated using k_{off} rate constants and dissociation constants obtained from ITC. [f]Not available.

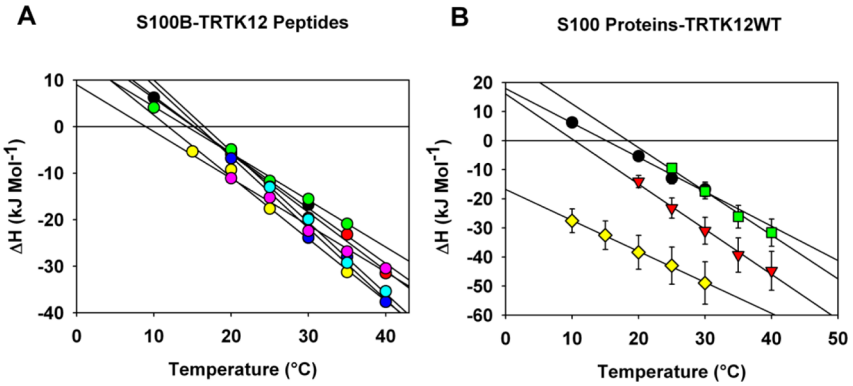

Figure 3. Temperature dependence of the enthalpies of binding, ΔH_{cal}. (A) Binding of TRTK12WT (black circles), TRTK12M1 (red circles), TRTKM5 (green circles), TRTKM6 (yellow circles), TRTKM9 (blue circles), TRTKM10 (pink circles), and TRTKM11 (cyan circles) peptides to the S100B protein in the presence of 5 mM calcium. Solid lines represent linear fits of the ΔH_{cal} temperature dependencies for each peptide−S100B interaction. The slopes of these lines represent the changes in heat capacity, which are summarized in Table 1. (B) Temperature dependence of the enthalpies, ΔH_{cal}, of the TRTK12WT peptide binding to S100B (circles), S100A1 (triangles), S100A2 (squares), and S100P (diamonds) in the presence of 5 mM calcium chloride.

Table 2. Summary of the Dissociation Constants, Changes in Heat Capacity upon Binding, and Kinetic Rate Constants of the TRTK12 Wild-Type Peptide and Alanine Variants Binding to S100A1 at 25 °C

peptide	K_d[a] (μM)	$\Delta C_{p,exp}$[b] (kJ mol^{-1} K^{-1})	$\Delta C_{p,calc}$[c] (kJ mol^{-1} K^{-1})	k_{off} (s^{-1})[d]	k_{on} ($\times 10^7$ M^{-1} s^{-1})[e]
TRTK12	3.4 ± 1.0 (1 ± 0.5)	−1.6 ± 0.1	−1.0 ± 0.1 (−1.6 ± 0.1)	44 ± 8	1.2 ± 0.3
TRTKM1	1.0 ± 0.2 (0.5 ± 0.1)	−2.0 ± 0.1	−0.7 ± 0.1 (−1.4 ± 0.1)	6 ± 2[f]	0.6 ± 0.2[f]
TRTKM5	11.7 ± 1.0 (6 ± 2)	−1.7 ± 0.2	−0.7 ± 0.1 (−1.5 ± 0.1)	77 ± 22	0.7 ± 0.2
TRTKM6	5.3 ± 3.0 (7 ± 3)	−2.2 ± 0.1	−0.9 ± 0.1 (−1.7 ± 0.1)	87 ± 13	1.6 ± 1.0
TRTKM9	3.1 ± 1.0 (0.6 ± 0.1)	−1.5 ± 0.1	−1.4 ± 0.1 (−1.7 ± 0.1)	97 ± 21[g]	2.7 ± 0.8[g]
TRTKM10	9.9 ± 1.0 (27 ± 15)	−1.7 ± 0.1	−0.7 ± 0.1 (−1.3 ± 0.1)	63 ± 6[g]	1.7 ± 0.4[g]
TRTKM11	4.5 ± 1.9 (2 ± 1)	−1.5 ± 0.1	−1.3 ± 0.1 (−1.5 ± 0.1)	71 ± 12	1.6 ± 0.7

[a]Dissociation constants obtained using ITC. Values in parentheses were obtained using emission fluorescence assays. [b]Experimentally determined changes in heat capacity upon binding (Figure 3). [c]Structure-based calculations (see eq 7) from homology models based on the human S100A1 dimer binding to two peptides using PDB entry 2KBM[32] or 3IQQ.[44] [d]k_{off} values obtained using fluorescence stopped-flow spectroscopy (eq 8). [e]k_{on} values calculated using k_{off} rate constants and dissociation constants obtained from ITC. [f]The k_{off} value was measured at 5 °C. The k_{on} value was calculated for the corresponding temperature. [g]The k_{off} value was measured at 15 °C. The k_{on} value was calculated for the corresponding temperature.

S100B dimer (eq 1; n = 1) and therefore is inaccurately represented by the homology models.

Steady-state emission fluorescence and fluorescence anisotropy were used to monitor protein−peptide binding and determine the dissociation constants as methods complementary to ITC. The TRTK12 peptides contain a tryptophan at position 7 (W7), which is buried in a hydrophobic binding pocket in the available structures.[29,32,43,44] This burial would be expected to lead to changes in the fluorescence intensity of W7 upon binding because of changes in the polarity of the chemical environment. The S100 proteins, with the exception of S100A1, do not contain a tryptophan and therefore contribute minimally to the overall signal intensity. The K_d obtained at 25 °C using fluorescence anisotropy for binding of the wild-type peptide to S100B (3 ± 1 μM) is in good agreement with that obtained from ITC (1.7 ± 0.1 μM). A similar correspondence in the binding affinities is observed for all alanine variants (Table 1).

Changes in fluorescence intensity using stopped-flow experiments were also used to monitor the k_{off} rates for peptide dissociation (see Experimental Procedures). In these experi-

dx.doi.org/10.1021/bi400788s | Biochemistry 2013, 52, 5844−5856

ments, the addition of EDTA to a preformed complex of an S100 protein and the TRTK12 peptides leads to calcium chelation and peptide dissociation. This dissociation is manifested as a change in fluorescence intensity. The emission fluorescence relaxation for peptide dissociation fit well to a single exponential as described by eq 8. The apparent k_{off} rate obtained for the dissociation of the wild-type TRTK12 peptide from S100B at 35 °C (86 ± 8 s^{-1}) is in good agreement with the previously obtained value from line-shape analysis of chemical shift changes monitored by NMR.[50] The kinetic rate constants for the interactions of S100B with all of the TRTK12 peptides are summarized in Table 1. There is only a 2-fold difference in the apparent k_{off} rates between the fastest and slowest peptides, consistent with the narrow range of K_d values observed for the alanine variants in ITC experiments.

Interactions of TRTK12 Peptides with S100A1. Figure 2B shows the binding isotherm obtained from ITC experiments at 25 °C in which the wild-type TRTK12 peptide was titrated into S100A1 in the presence of 5 mM $CaCl_2$. As with S100B, the stoichiometry of the interaction is two TRTK12 peptides per S100A1 dimer (eq 1; n = 2). The dissociation constant obtained from the fit was found to be 3.4 ± 1.0 μM (Table 2), which is weaker than that of the S100B-TRTK12 interaction (Table 1), consistent with a previous report of S100A1 binding this peptide with a 2-fold reduced affinity.[7] For the TRTK12 alanine variants, the interactions between S100A1 and a given TRTK12 peptide are also characterized by weaker binding affinities, when compared to those of S100B and the same peptide. This trend is apparent in the dissociation constants measured by both ITC and emission fluorescence (Table 2). In particular, the TRTKM5 peptide binds to S100A1 with a 10-fold weaker affinity than to S100B. Overall, there is also a larger variation within the binding affinities of the TRTK12 peptides for S100A1, as compared to those for S100B.

Figure 3B shows the comparison of the enthalpies of binding of the TRTK12 wild-type peptide to different S100 proteins, including S100A1 and S100B. The absolute values of the enthalpies for S100A1 are significantly lower than those for S100B. The temperature dependence of the enthalpies, which represent ΔC_p, is also somewhat different for these proteins (Table 2). For the binding of the alanine variants to S100A1, the ΔC_p values also differ from the binding of the wild type. In particular, binding of the TRTKM6 peptide shows the largest ΔC_p value (Table 2). Structure-based calculations of the changes in heat capacity are listed in Table 2. A comparison shows that, in general, the calculated values are close to the experimentally determined ΔC_p values for the binding of the TRTK12 peptides to S100A1. However, the best agreement appears to be with the homology models derived from X-ray structures of the S100B−TRTK12 complex from the Weber group,[44] as opposed to those derived from rat S100A1.[32]

Table 2 summarizes the dissociation constants and kinetic rate constants for the peptide binding to S100A1. As with S100B, all peptides fit well to a single exponential, consistent with the binding model of two peptides per S100B dimer (eq 1; n = 2). The apparent k_{off} rates are faster than those observed for S100B, suggesting a compensatory effect in the off rate to account for the weaker binding affinities. For both proteins, the kinetics and dissociation constants for all peptides differ by ≤1 order of magnitude.

Interactions of TRTK12 Peptides with S100A2. The binding of TRTK12 to human S100A2 is a novel interaction, which was identified by us using tryptophan fluorescence and was further confirmed using ITC. Figure 2C shows the binding isotherm obtained from ITC experiments at 25 °C in which the wild-type TRTK12 peptide was titrated into S100A2 in the presence of 5 mM $CaCl_2$. Although the binding model for the wild-type peptide is consistent with both S100B and S100A1 (eq 1; n = 2), the dissociation constant is >1 order of magnitude weaker (48 ± 3 μM). Similarly, the dissociation constants for the binding of the TRTK12 alanine variants to S100A2 are significantly weaker than those for both S100B and S100A1 (Table 3). Notably, the TRTKM5 and TRTKM11 peptides bind to S100A2 with a much weaker affinity than the wild type, 3- and 10-fold, respectively. Furthermore, the TRTKM10 peptide, which substitutes a C-terminal isoleucine for an alanine, exhibits no detectable binding by ITC or emission fluorescence (data not shown). As with S100A1, the TRTKM1 peptide appears to bind more tightly to S100A2 than does the wild type. In addition, the experimentally determined ΔC_p values of the alanine variants are generally smaller than those of either S100B or S100A1 (Table 3). This possibly indicates that a smaller amount of hydrophobic surface area is buried in the bound state of the S100A2−TRTK12WT complex, although a compensatory effect in the hydrophilic surface area cannot be ruled out until a structure of the bound complex becomes available. There are large deviations in the heat capacity upon binding of the TRTK12 alanine variants to S100A2, relative to both the wild type and the calculated values based on a variety of structural models (Table 3). This suggests several of the alanine variants may adopt different conformations in the bound complex relative to the wild-type peptide.

Table 3. Summary of the Dissociation Constants and Changes in the Heat Capacity upon Binding of the TRTK12 Wild-Type Peptide and Alanine Variants Binding to S100A2 at 25 °C

peptide	K_d[a] (μM)	$\Delta C_{p,exp}$[b] (kJ mol^{-1} K^{-1})	$\Delta C_{p,calc}$[c] (kJ mol^{-1} K^{-1})
TRTK12	48 ± 3 (43 ± 9)	−1.5 ± 0.1	−1.5 ± 0.1
TRTKM1	15.2 ± 1.0 (16 ± 1)	−0.8 ± 0.1	−1.3 ± 0.1
TRTKM5	131.0 ± 6.1 (N/A)[c]	−0.9 ± 0.1	−1.3 ± 0.1
TRTKM6	21.5 ± 4.0 (23 ± 3)	−0.7 ± 0.1	−1.5 ± 0.1
TRTKM9	45.0 ± 2.0 (17 ± 4)	−0.4 ± 0.1	−1.5 ± 0.1
TRTKM10[d]	–	–	–
TRTKM11	504 ± 9.7 (N/A)[c]	−1.6 ± 0.1	−1.5 ± 0.1

[a]Dissociation constants obtained using ITC. Values in parentheses were obtained using emission fluorescence assays. [b]Experimentally determined changes in heat capacity upon binding (Figure 3). [c]Structure-based calculations (see eq 7) from homology models based on the human S100A2 dimer binding to two peptides using PDB entry 3IQQ.[44] [d]No detectable binding by ITC or emission fluorescence.

We were unable to measure the dissociation rate constants for any TRTK12 peptide from S100A2 because there was no detectable change in the emission fluorescence intensity upon the addition of EDTA. Dynamic quenching assays with acrylamide confirmed that W7 of the TRTK12 peptides is buried in the bound complex with S100A2 to a similar extent as with other proteins, such as S100B (Table 4). Furthermore, there are no detectable heats of binding for the TRTK12 peptide and S100A2 in the absence of calcium, which suggests

Table 4. Stern–Volmer (K_{SV}) Constants of the TRTK12 Peptides in the Free and Bound States for Various Complexes with S100B, S100A2, and S100P

	peptide only K_{SV} (M^{-1})	S100B/peptide K_{SV} (M^{-1})	S100A2/peptide K_{SV} (M^{-1})	S100P/peptide K_{SV} (M^{-1})
TRTK12	14.0 ± 0.2	2.1 ± 0.1[a]	4.9 ± 0.5[a]	8.5 ± 0.2
TRTKM1	14.9 ± 0.2	2.4 ± 0.1	4.3 ± 0.2	nd[b]
TRTKM5	11.9 ± 1.0	2.8 ± 0.1	8.9 ± 0.2	11.2 ± 0.2
TRTKM6	11.8 ± 0.2	3.7 ± 0.1[a]	4.7 ± 0.1[a]	11.3 ± 0.3
TRTKM9	15.4 ± 0.2	7.2 ± 0.2	6.1 ± 1.1	13.6 ± 0.4
TRTKM10	13.6 ± 0.3	7.5 ± 0.1	nd[b]	nd[b]
TRTKM11	13.8 ± 0.1	7.2 ± 0.1	8.7 ± 0.2	nd[b]

[a]Experiments performed in the presence of 150 mM NaCl. [b]Not determined.

that there is no calcium-independent binding. On the basis of these findings, we conclude that the off rates themselves are too fast to be detected by the stopped-flow instrument (instrument dead time of 4 ms). This places the lower bound of k_{off} at 250 s^{-1} and results in k_{on} rates that are equal to or less than those of S100B.

Interactions of TRTK12 Peptides with S100P. The binding of wild-type TRTK12 with S100P is the only other novel interaction identified for this peptide and the human S100 proteins. Figure 2D shows a typical titration of the TRTK12 peptide into S100P. The dissociation constant (5.1 ± 1.0 μM) is weaker than that of S100B and S100A1, but the binding is still significantly tighter than that of S100A2 (Table 5). As with S100A2, the TRTKM5 and TRTKM10 peptides exhibit substantially reduced affinities, while the TRTKM11 peptide binds with a similar stoichiometry to S100B [one peptide per S100P dimer (eq 1; $n = 1$)]. This stoichiometry has previously been observed for several peptides binding to the S100 proteins,[63] most notably to S100B,[50,68] S100A4,[65−67,69] and S100A10.[65−67] The results obtained for the TRTKM11 peptide suggest significant plasticity in peptide binding and show an interesting case in which a single-amino acid substitution can switch between different binding modes. The difference in the affinities does not correlate with the differences in the enthalpies of binding; i.e., there is no enthalpy−entropy compensation (data not shown). In addition, there were no observable changes in the emission fluorescence intensity of the tryptophan upon peptide binding or dissociation to S100P for three of the alanine variants: TRTKM5, TRTKM6, and TRTKM9. This suggests that there may be an alternate mode of binding for these peptides in which W7 is solvent-exposed in the bound complex. Dynamic quenching with acrylamide was used to probe the relative exposure of W7. Judging by the similarity between the Stern−Volmer constants of the S100P−TRTK12 peptide complexes and the free TRTK12 peptides (Table 4), we conclude that W7 is indeed exposed in the TRTKM5, TRTKM6, and TRTKM9 complexes with S100P.

The absolute enthalpies of binding of the TRTK12 wild-type peptide to S100P are significantly lower than those of the other S100 proteins, including S100A1 (Figure 3B). However, the changes in heat capacity upon binding, ΔC_p, are very similar to those of S100B (Table 5). As with S100B, the ΔC_p values for the binding of the alanine variants to S100P are generally within error of those of the wild type. The only notable exception is TRTKM11, which binds with a different stoichiometry (see above). This suggests that the TRTKM5, TRTKM6, and TRTKM9 variants bind in a manner that compensates for the exposure of W7, possibly by burying other hydrophobic residues in the bound complex.

Because there are no changes in the emission fluorescence intensity for TRTKM5, TRTKM6, and TRKTM10 peptides, the kinetic rate constants of binding to S100P could only be measured for the remaining TRTK12 peptides (Table 5). Although it is a limited data set, the measured k_{off} rates are the fastest observed among the other studied S100 proteins.

DISCUSSION

Promiscuity of the S100B-Binding Site. Since its discovery in 1965, S100B has become the best-studied member of the S100 protein family.[70] To date, more than 20 binding partners have been identified, including p53, RAGE, tau, NDR, microtubules, intermediate filaments, GFAP, and CapZ (TRTK12).[10,40−42,44,45,50,71−74] Despite the promising work of Ivanenkov et al. to elucidate a target binding motif,[35,46] subsequent studies have revealed a large degree of promiscuity within the S100B-binding pocket and significant variability within the consensus binding sequence.[50,71,75] In particular, recent work by Weber et al. suggests that no particular residue or position from the original phage display motif, (K/R)-(L/I)-X-W-X-I-L, is a prerequisite for binding.[71] Indeed, the only characteristics shared by all available binding partners are the

Table 5. Summary of the Dissociation Constants, Changes in Heat Capacity upon Binding, and Kinetic Rate Constants of the TRTK12 Wild-Type Peptide and Alanine Variants Binding to S100P at 25 °C

peptide	K_d[a] (μM)	$\Delta C_{p,exp}$[b] (kJ mol^{-1} K^{-1})	$\Delta C_{p,calc}$[c] (kJ mol^{-1} K^{-1})	k_{off} (s^{-1})[d]	k_{on} ($\times 10^7$ M^{-1} s^{-1})[e]
TRTK12	5.1 ± 0.3 (11 ± 1)	−1.1 ± 0.1	−1.7 ± 0.1	286 ± 43[f]	5.6 ± 0.9[f]
TRTKM1	1.0 ± 0.5 (7 ± 3)	−0.9 ± 0.1	−1.4 ± 0.1	135 ± 18	6.8 ± 1.9
TRTKM5	56.2 ± 4.0 (100 ± 23)	−1.2 ± 0.1	−1.5 ± 0.1	–	–
TRTKM6	7.4 ± 1.0 (16 ± 4)	−0.9 ± 0.1	−1.6 ± 0.1	–	–
TRTKM9	7.1 ± 0.5 (30 ± 10)	−1.0 ± 0.1	−1.7 ± 0.1	–	–
TRTKM10	43.1 ± 3.9 (not determined)	−1.3 ± 0.1	−1.3 ± 0.1	32 ± 11[g]	0.07 ± 0.03[g]
TRTKM11	31.7 ± 0.5 (not determined)	−1.8 ± 0.1	−1.5 ± 0.1	151 ± 25[h]	0.6 ± 0.1[h]

[a]Dissociation constants obtained using ITC. Values in parentheses were obtained using emission fluorescence assays. [b]Experimentally determined changes in heat capacity upon binding (Figure 3). [c]Structure-based calculations (see eq 7) using the average value from homology models based on the human S100P dimer binding to two peptides using PDB entry 3IQQ.[44] [d]k_{off} value obtained using fluorescence stopped-flow spectroscopy (eq 8). [e]k_{on} values were calculated using the k_{off} rate constants and the dissociation constants obtained from ITC. [f]The k_{off} value is within error of the dead time but is consistent with the temperature-dependent slope of the rate constant. [g]The k_{off} value was measured at 5 °C. The k_{on} value was calculated for the corresponding temperature. [h]The k_{off} value was measured at 20 °C. The k_{on} value was calculated for the corresponding temperature.

dx.doi.org/10.1021/bi400788s | Biochemistry 2013, 52, 5844−5856

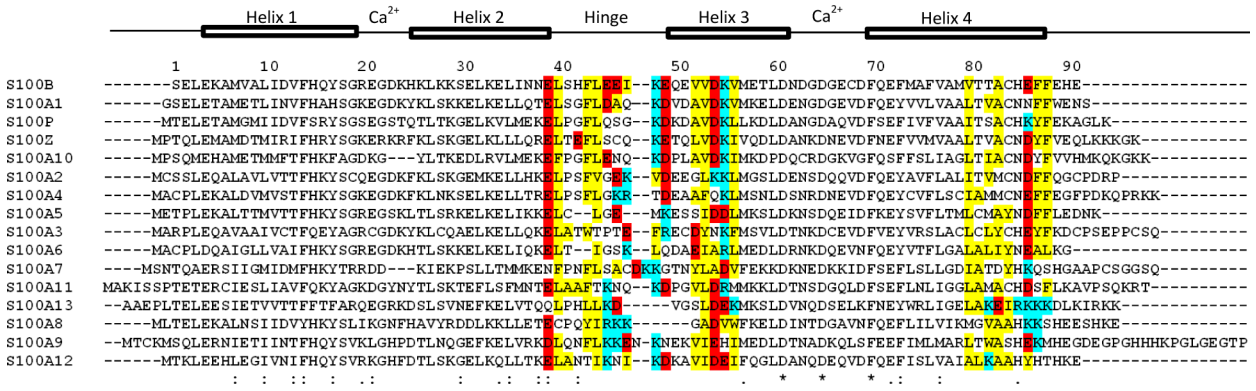

Figure 4. Sequence comparison of human S100 proteins. Sequence alignment of human S100 family members generated using ClustalOmega.[106] For the sake of clarity, residue numbering in the text is always written in reference to the sequence of S100B.

presence of several hydrophobic residues and at least one intervening positive residue. This suggests that the binding affinity of TRTK12 for S100B is probably dominated by nonspecific, hydrophobic interactions and modulated by only electrostatic interactions. These minimal requirements for binding S100B may explain why it is able to interact with different targets through novel binding modes, with variations in stoichiometry, affinity, and cooperativity.[50,71,76]

The assessment described above is consistent with the results of this study, in which no single-alanine mutation of the TRTK12 peptide significantly altered the binding affinity or kinetics [observed changes in K_d and k_{off} are <2-fold (see Table 1)]. This includes the charge-neutralizing variants, TRTKM6 and TRTKM9, which contain D6A and K9A substitutions, respectively. These results are consistent with the original phage display assay, which found no amino acid preference for position 6 within the TRTK12 sequence and no preference for a positively charged residue flanking the C-terminal side of the tryptophan (i.e., residue 9).[35] Furthermore, the presence of physiological salt concentration had no observable effect on the dissociation constant of the wild-type peptide and caused only a slight decrease in the apparent k_{off} (data not shown). Because the TRTK12 alanine variants appear to only slightly modulate the peptide binding affinity, our findings suggest that the tryptophan (W7) acts as a bulky hydrophobic anchor for the TRTK12 peptide binding to S100B, consistent with previous proposals.[43,71,77]

The W7 of TRTK12 may also play an important role in the kinetics of peptide binding. It has previously been proposed that S100B interacts with several of its binding partners through a "fly-casting mechanism", in which the peptide remains unstructured in a "low-affinity" encounter complex and proceeds to adopt a folded conformation in the final "high-affinity" complex.[50,78,79] This model is increasingly being examined as a rational explanation for the promiscuity of S100B because so many of its binding partners appear to be unstructured in the unbound state.[50,77,78] Furthermore, computational models suggest that several binding partners of S100B form initial contacts via a large, nonpolar residue, such as a tryptophan or phenylalanine.[77,78] The underlying principle is that intrinsically disordered proteins or peptides (IDP), such as TRTK12, have a larger "capture radius" than peptides with a preformed structure[80] and therefore increase the bimolecular association rates.[81] A recent review by Kiefhaber et al. quantitatively defined the fly-casting mechanism as a bimolecular association involving an IDP with an apparent k_{on} rate of $\geq 1 \times 10^7$ M^{-1} s^{-1}.[82] This mechanism is consistent with the association rate constants observed for the TRTK12 peptides binding to S100B (Table 1), and the observed changes in the conformational ensemble of the peptide between the free and bound states.[40,41,44,50]

TRTK12 Selectively Binds a Subset of S100 Proteins. Previously, it has been suggested that TRTK12 binds to several, distantly related members of the S100 family and therefore represents a general S100-binding motif.[32] In contrast, the results of this study indicate that TRTK12 selectively binds S100B and only three other S100 proteins: S100A1, S100P, and S100A2. The available structures of the TRTK12 peptide bound to S100B and S100A1,[29,32,43,44] as well as the sequence alignment of the S100 proteins, suggest a rational basis for the specificity of binding observed in this study. A phylogenetic analysis of the S100 family indicates that two of these proteins, S100A1 and S100P, are the members most closely related to S100B (Figure 5), consistent with the similar affinities and kinetics observed for wild-type TRTK12 binding (Tables 1, 2, and 5). Furthermore, S100A1 exhibits an insensitivity to alanine mutagenesis similar to that of S100B (Table 2) and also appears to interact with an equally large and diverse set of binding partners.[75] These similarities are most likely due to not only the global homology between S100A1 and S100B but also the sequence conservation within the hinge and C-terminal helix regions (Figure 4). Previous bioinformatics studies have revealed that the hinge and C-terminal helix regions of the S100 proteins contain the largest degree of sequence variability, and a number of crystallographic and solution structures have demonstrated these regions are crucial for S100 target recognition.[6,30,32,42,50,83−86] The composite binding sites for S100B−TRTK12 and S100A1−TRTK12 complexes differ significantly only in terms of their charge distributions. Lys58 of S100A1 has no homologous residue in S100B, and Asp86 of S100B is replaced with an asparagine in the S100A1 sequence. These substitutions may be sufficient to explain the 2-fold weaker binding affinity of the wild-type peptide for S100A1 in the presence of a physiological ionic strength (data not shown).

A hydrophobic pocket for W7 of TRTK12 in the structure of the S100B−peptide complex is formed by several residues, including I36, L44, V52, and V56. The corresponding positions in the sequence of S100A1 are L36, L44, A52, and V56, respectively (Figure 4). Many of the residues that form the binding pocket in the S100B−TRTK12 and S100A1−TRTK12 complexes are not conserved in other S100 proteins. This sequence difference likely leads to the increased sensitivity of

dx.doi.org/10.1021/bi400788s | Biochemistry 2013, 52, 5844−5856

the TRTK12 alanine variants for S100A2 and S100P and the inability of most S100 proteins to bind the TRTK12 peptide. In the absence of structural information for TRTK12 complexes with S100P and S100A2, it is difficult to identify the "hot spots" that define the binding specificity. Therefore, one can provide only a possible rationale based on the sequence alignment. For example, within the hinge region of S100P, several substitutions change both the net polarity and charge, relative to those of S100B. These include S41P, E45Q, E46S, and Q50K substitutions. Several residues within helices III and IV have also been replaced, including V56L, M79A, and V80I substitutions that modify the shape of the hydrophobic pocket and are likely responsible for the reduced affinity of the TRTKM5, TRTKM10, and TRTKM11 variants for S100P. This may also explain why the TRTKM5, TRTKM6, and TRTKM9 alanine variants are still able to bind S100P, despite the apparent exposure of W7 to solvent (Table 4). Interestingly, S100A10 and S100Z, which are closely related to S100B, S100A1, and S100P, do not appear to interact with the TRTK12WT peptide (Table 1). This may be the result of nonconserved substitutions within the hinge region, including H42E, E45S, and I47Q substitutions in S100Z and I36M, I47Q, and V56I substitutions in S100A10. In addition, S100A10 and S100Z both have an unusually long, unstructured region following helix IV that consists of four Lys residues, which may electrostatically repulse the TRTK12 peptide and/or partially occlude the binding site.

S100A2 is the only member of the S100A2/S100A3/S100A4/S100A5/S100A6 phylogenetic branch that is able to bind TRTK12 (Figure 5). Furthermore, it appears to be the

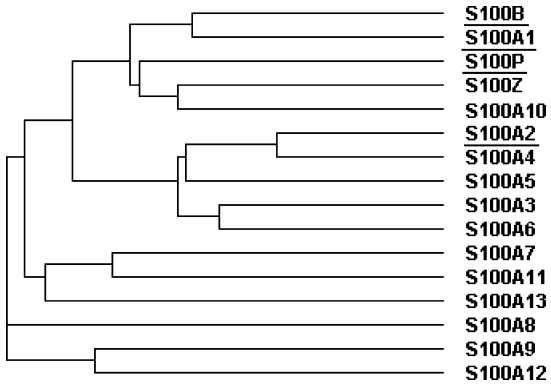

Figure 5. Phylogenetic tree based on the sequence alignment. For the sake of clarity, proteins that were found to interact with TRTK12 (S100B, S100A1, S100P, and S100A2) are underlined.

S100 protein most sensitive to the TRTK12 motif, as demonstrated by the ability of the TRKTM11 variant, which substitutes an alanine for isoleucine, to completely abolish binding. Similarly, the TRTKM5 and TRTKM11 variants, which contain I5A and L11A substitutions, respectively, bind S100A2 with significantly weaker affinities (Table 2). This is likely the result of key substitutions within the hinge (S41P, E45G, I47K, K48V, and Q50E) and C-terminal helices (V52L, V56L, and A83M)of S100A2, relative to those of S100B. A sequence comparison demonstrates that the other members of this phylogenetic branch contain significant variations in the number and type of charged residues in their hinge region, relative to those of S100B (Figure 4). In particular, they lack a number of conserved glutamic acid and aspartic acid residues, which may contribute to the inability of the positively charged TRTK12 peptide to bind to these proteins. Furthermore, S100A3 is believed to have a calcium dissociation constant of ≥30 mM, meaning that, within this study, the majority of the population would have remained in the apo state, with its hydrophobic binding site secluded.[87] S100A3 has been proposed to bind zinc with high affinity, which induces a conformational change similar to that observed for other S100 proteins in the presence of calcium, but the effects of Zn^{2+}-bound S100A3 were not probed in this study. S100A4 is similar to S100Z in that it has a large, positively charged unstructured region following the C-terminal helix. This region is thought to play an important role in the tetramerization of S100A4 by binding to the canonical binding site of an adjacent dimer,[88] but it may also fold back onto the protein surface and interfere with the binding sites within an individual dimer. S100A5 and S100A6 both contain a truncated hinge region, as demonstrated by their three- and two-residue gaps, respectively, relative to the other S100 proteins (Figure 4). In addition, the residues in this hinge region are not conserved, relative to those of S100B. A glycine occupies the position of Glu45 in both S100A5 and S100A6, and neither of the sequences contains His42, Phe43, or Ile47. The increased level of sequence divergence within the S100A2 subgroup, especially in terms of polar and charged residues, results in a binding pocket that is incompatible with the TRTK12 peptide.

Selective Inhibitions of S100 Proteins. Differential expression of individual S100 proteins has been implicated in a wide variety of aberrant cellular processes, making them prime candidates for therapeutic targeting.[1,4,5,23,75] However, each individual S100 protein has been associated with a variety of diverse, tissue-specific, and sometimes antagonistic functions. For example, upregulation of S100B has been observed in Alzheimer's disease,[7,8,10] Parkinson's disease,[11,89,90] Down's syndrome,[9] epilepsy,[91] melanoma,[23,92,93] and glioblastomas.[94] In contrast, downregulation of S100A1 is associated with an increased likelihood of cardiovascular disease and cardiomyopathies.[16,17] Upregulation of S100A2 has been shown to suppress tumor growth in certain epithelial tissues[95] but to promote metastasis within the lungs and cervix.[96,97] The interaction of S100 proteins with their cellular targets is further complicated by the ability of these proteins to localize and associate with other family members, such as in the S100B/S100A1 heterodimer,[98] and the ability of multiple S100 proteins to interact with the same binding partner, such as p53.[22,71,99] Therefore, there is a need to selectively inhibit individual S100 proteins, without detrimentally affecting the biological pathways of closely related homologues.

The results of this study indicate that single-point variants of the TRTK12 peptide are sufficient to selectively target S100B, or any subset of TRTK12 binding-competent S100 proteins that include S100B. For example, TRTKM1 exhibits 2−4-fold enhanced affinity for S100A1, S100A2, and S100P relative to the wild-type peptide, while binding to S100B remains unchanged. Thus, this peptide can putatively act as a micromolar inhibitor for binding of cellular targets for all four S100 proteins. Similarly, the wild-type or TRTKM9 peptides can be used to selectively inhibit S100B, S100A1, and S100P and not S100A2, because S100A2 binds these peptides 1 order of magnitude more weakly (Table 3). Likewise, the TRTKM11 peptide can be used to preferentially bind S100B and S100A1, as opposed to S100A2 or S100P. Finally, the TRTKM5 peptide can be used to selectively inhibit only S100B

as the dissociation constants for S100A1, S100P, and S100A2 for this peptide are 1−2 orders of magnitude weaker than that for S100B.

These *in vitro* results suggest a potential strategy for targeting S100 proteins with individual, peptide-based inhibitors. However, ideal drug candidates usually require nanomolar efficacy *in vivo*,[100] as opposed to the micromolar dissociation constants observed in this study. Furthermore, peptides have traditionally been avoided as therapeutic candidates because of their low bioavailability, decreased membrane permeability, and high likelihood of degradation and clearance by the cellular machinery.[101] Nonetheless, several groups have recently published work demonstrating that these drawbacks can be overcome by stabilizing peptides using "hydrocarbon staples".[102] In several cases, these peptides exhibit enhanced binding affinity, as well as increased cell permeability and resistance to degradation.[101−105] In particular, they have shown promise as cancer therapeutics by binding to previously "undruggable" targets, such as members of the pro-survivor BL-2 family or HDMX/MDMX apoptotic proteins.[103,105] The S100 proteins derived from the A1/A11/B/P/Z and A2/A3/A4/A5/A6 subgroups have been proposed to directly and indirectly regulate these pathways through interactions with the p53, HDM2, and HDM4 proteins.[50,71,76] In particular, S100B is currently the best biological prognosticator for malignant melanoma, with serum concentrations of the protein inversely proportional to long-term survival rates.[93] This suggests that a modified TRTK12 peptide may represent a promising starting point for an *in vivo* inhibitor of S100B and/or related S100 proteins. In addition, the small size of the TRTK12 peptide and low sensitivity of its binding to ionic strength are advantageous in comparison to other binding partners of S100B, such as the C-terminus of p53. The ability to individually inhibit homologous proteins, with similar sequences and tertiary structures, represents an important step toward rational drug design.

■ ASSOCIATED CONTENT

Supporting Information

Three additional figures providing details on stopped-flow, fluorescence anisotropy, and fluorescence quenching. This material is available free of charge via the Internet at http://pubs.acs.org.

■ AUTHOR INFORMATION

Corresponding Author

*Center for Biotechnology and Interdisciplinary Studies, Rensselaer Polytechnic Institute, 110 Eighth St., Troy, NY 12180. E-mail: makhag@rpi.edu. Telephone: (518) 276-4417. Fax: (518) 276-2955.

Funding

This work was supported by the National Institute of General Medical Sciences Grant RO1-GM054537.

Notes

The authors declare no competing financial interest.

■ ACKNOWLEDGMENTS

Instrumentation at the Core Facilities at the Center of Biotechnology and Interdisciplinary Studies at Rensselaer Polytechnic Institute was used for some of the experiments reported in this paper. We thank Dr. Werner Streicher for his guidance and insights.

■ ABBREVIATIONS

ITC, isothermal titration calorimetry; EF-hand, calcium-binding domain consisting of a helix−loop−helix structure; Fmoc, fluorenylmethyloxycarbonyl chloride; TCEP, tris(2-carboxyethyl)phosphine; PDB, Protein Data Bank.

■ REFERENCES

(1) Schafer, B. W., and Heizmann, C. W. (1996) The S100 family of EF-hand calcium-binding proteins: Functions and pathology. *Trends Biochem. Sci. 21*, 134−140.

(2) Deloulme, J. C., Mbele, G. O., and Baudier, J. (2002) S100 proteins. From purification to functions. *Methods Mol. Biol. 172*, 185−198.

(3) Donato, R. (2001) S100: A multigenic family of calcium-modulated proteins of the EF-hand type with intracellular and extracellular functional roles. *Int. J. Biochem. Cell Biol. 33*, 637−668.

(4) Donato, R. (1999) Functional roles of S100 proteins, calcium-binding proteins of the EF-hand type. *Biochim. Biophys. Acta 1450*, 191−231.

(5) Donato, R. (2003) Intracellular and extracellular roles of S100 proteins. *Microsc. Res. Tech. 60*, 540−551.

(6) Marenholz, I., Heizmann, C. W., and Fritz, G. (2004) S100 proteins in mouse and man: From evolution to function and pathology (including an update of the nomenclature). *Biochem. Biophys. Res. Commun. 322*, 1111−1122.

(7) Chaves, M. L., Camozzato, A. L., Ferreira, E. D., Piazenski, I., Kochhann, R., Dall'igna, O., Mazzini, G. S., Souza, D. O., and Portela, L. V. (2010) Serum levels of S100B and NSE proteins in Alzheimer's disease patients. *J. Neuroinflammation 7*, 6−7.

(8) Anderson, P. J., Watts, H. R., Jen, S., Gentleman, S. M., Moncaster, J. A., Walsh, D. T., and Jen, L. S. (2009) Differential effects of interleukin-1β and S100B on amyloid precursor protein in rat retinal neurons. *Clin. Ophthalmol. 3*, 235−242.

(9) Esposito, G., Imitola, J., Lu, J., De Filippis, D., Scuderi, C., Ganesh, V. S., Folkerth, R., Hecht, J., Shin, S., Iuvone, T., Chesnut, J., Steardo, L., and Sheen, V. (2008) Genomic and functional profiling of human Down syndrome neural progenitors implicates S100B and aquaporin 4 in cell injury. *Hum. Mol. Genet. 17*, 440−457.

(10) Leclerc, E., Sturchler, E., and Vetter, S. W. (2010) The S100B/RAGE Axis in Alzheimer's Disease. *Cardiovasc. Psychiatry Neurol. 2010*, 539−581.

(11) Liu, J., Wang, H., Zhang, L., Xu, Y., Deng, W., Zhu, H., and Qin, C. (2011) S100B transgenic mice develop features of Parkinson's disease. *Arch. Med. Res. 42*, 1−7.

(12) Goyette, J., and Geczy, C. L. (2011) Inflammation-associated S100 proteins: New mechanisms that regulate function. *Amino Acids 41*, 821−842.

(13) Foell, D., Wittkowski, H., Vogl, T., and Roth, J. (2007) S100 proteins expressed in phagocytes: A novel group of damage-associated molecular pattern molecules. *J. Leukocyte Biol. 81*, 28−37.

(14) Foell, D., Wittkowski, H., Ren, Z., Turton, J., Pang, G., Daebritz, J., Ehrchen, J., Heidemann, J., Borody, T., Roth, J., and Clancy, R. (2008) Phagocyte-specific S100 proteins are released from affected mucosa and promote immune responses during inflammatory bowel disease. *J. Pathol. 216*, 183−192.

(15) Kaiser, T., Langhorst, J., Wittkowski, H., Becker, K., Friedrich, A. W., Rueffer, A., Dobos, G. J., Roth, J., and Foell, D. (2007) Faecal S100A12 as a non-invasive marker distinguishing inflammatory bowel disease from irritable bowel syndrome. *Gut 56*, 1706−1713.

(16) Remppis, A., Greten, T., Schafer, B. W., Hunziker, P., Erne, P., Katus, H. A., and Heizmann, C. W. (1996) Altered expression of the Ca^{2+}-binding protein S100A1 in human cardiomyopathy. *Biochim. Biophys. Acta 1313*, 253−257.

(17) Rohde, D., Ritterhoff, J., Voelkers, M., Katus, H. A., Parker, T. G., and Most, P. (2010) S100A1: A multifaceted therapeutic target in cardiovascular disease. *Journal of Cardiovascular Translational Research 3*, 525−537.

(18) Tarabykina, S., Scott, D. J., Herzyk, P., Hill, T. J., Tame, J. R., Kriajevska, M., Lafitte, D., Derrick, P. J., Dodson, G. G., Maitland, N. J., Lukanidin, E. M., and Bronstein, I. B. (2001) The dimerization interface of the metastasis-associated protein S100A4 (Mts1): In vivo and in vitro studies. *J. Biol. Chem. 276*, 24212−24222.
(19) Gibadulinova, A., Tothova, V., Pastorek, J., and Pastorekova, S. (2010) Transcriptional regulation and functional implication of S100P in cancer. *Amino Acids 41*, 885−892.
(20) Takenaga, K., Nakamura, Y., Endo, H., and Sakiyama, S. (1994) Involvement of S100-related calcium-binding protein pEL98 (or mts1) in cell motility and tumor cell invasion. *Jpn. J. Cancer Res. 85*, 831−839.
(21) Nakazato, Y., Ishizeki, J., Takahashi, K., and Yamaguchi, H. (1982) Immunohistochemical localization of S-100 protein in granular cell myoblastoma. *Cancer 49*, 1624−1628.
(22) Mueller, A., Schafer, B. W., Ferrari, S., Weibel, M., Makek, M., Hochli, M., and Heizmann, C. W. (2005) The calcium-binding protein S100A2 interacts with p53 and modulates its transcriptional activity. *J. Biol. Chem. 280*, 29186−29193.
(23) Salama, I., Malone, P. S., Mihaimeed, F., and Jones, J. L. (2008) A review of the S100 proteins in cancer. *European Journal of Surgical Oncology 34*, 357−364.
(24) Botelho, H. M., Fritz, G., and Gomes, C. M. (2012) Analysis of s100 oligomers and amyloids. *Methods Mol. Biol. 849*, 373−386.
(25) Streicher, W. W., Lopez, M. M., and Makhatadze, G. I. (2010) Modulation of quaternary structure of S100 proteins by calcium ions. *Biophys. Chem. 151*, 181−186.
(26) Lee, Y. C., Volk, D. E., Thiviyanathan, V., Kleerekoper, Q., Gribenko, A. V., Zhang, S., Gorenstein, D. G., Makhatadze, G. I., and Luxon, B. A. (2004) NMR structure of the Apo-S100P protein. *J. Biomol. NMR 29*, 399−402.
(27) Dempsey, A. C., Walsh, M. P., and Shaw, G. S. (2003) Unmasking the annexin I interaction from the structure of apo-S100A11. *Structure 11*, 887−897.
(28) Wright, N. T., Inman, K. G., Levine, J. A., Cannon, B. R., Varney, K. M., and Weber, D. J. (2008) Refinement of the solution structure and dynamic properties of Ca^{2+}-bound rat S100B. *J. Biomol. NMR 42*, 279−286.
(29) Wright, N. T., Varney, K. M., Ellis, K. C., Markowitz, J., Gitti, R. K., Zimmer, D. B., and Weber, D. J. (2005) The three-dimensional solution structure of Ca^{2+}-bound S100A1 as determined by NMR spectroscopy. *J. Mol. Biol. 353*, 410−426.
(30) Lee, Y. T., Dimitrova, Y. N., Schneider, G., Ridenour, W. B., Bhattacharya, S., Soss, S. E., Caprioli, R. M., Filipek, A., and Chazin, W. J. (2008) Structure of the S100A6 complex with a fragment from the C-terminal domain of Siah-1 interacting protein: A novel mode for S100 protein target recognition. *Biochemistry 47*, 10921−10932.
(31) Bertini, I., Das Gupta, S., Hu, X., Karavelas, T., Luchinat, C., Parigi, G., and Yuan, J. (2009) Solution structure and dynamics of S100A5 in the apo and Ca^{2+}-bound states. *JBIC, J. Biol. Inorg. Chem. 14*, 1097−1107.
(32) Wright, N. T., Cannon, B. R., Wilder, P. T., Morgan, M. T., Varney, K. M., Zimmer, D. B., and Weber, D. J. (2009) Solution structure of S100A1 bound to the CapZ peptide (TRTK12). *J. Mol. Biol. 386*, 1265−1277.
(33) Zimmer, D. B., and Van Eldik, L. J. (1989) Analysis of the calcium-modulated proteins, S100 and calmodulin, and their target proteins during C6 glioma cell differentiation. *J. Cell Biol. 108*, 141−151.
(34) Selinfreund, R. H., Barger, S. W., Pledger, W. J., and Van Eldik, L. J. (1991) Neurotrophic protein S100β stimulates glial cell proliferation. *Proc. Natl. Acad. Sci. U.S.A. 88*, 3554−3558.
(35) Ivanenkov, V. V., Jamieson, G. A., Jr., Gruenstein, E., and Dimlich, R. V. (1995) Characterization of S-100b binding epitopes. Identification of a novel target, the actin capping protein, CapZ. *J. Biol. Chem. 270*, 14651−14658.
(36) Henzl, M. T., Davis, M. E., and Tan, A. (2008) Leucine 85 is an important determinant of divalent ion affinity in rat β-parvalbumin (oncomodulin). *Biochemistry 47*, 13635−13646.
(37) Henzl, M. T., and Tanner, J. J. (2007) Solution structure of Ca^{2+}-free rat β-parvalbumin (oncomodulin). *Protein Sci. 16*, 1914−1926.
(38) Henzl, M. T., and Tanner, J. J. (2008) Solution structure of Ca^{2+}-free rat α-parvalbumin. *Protein Sci. 17*, 431−438.
(39) Rezvanpour, A., Phillips, J. M., and Shaw, G. S. (2009) Design of high-affinity S100-target hybrid proteins. *Protein Sci. 18*, 2528−2536.
(40) Inman, K. G., Yang, R., Rustandi, R. R., Miller, K. E., Baldisseri, D. M., and Weber, D. J. (2002) Solution NMR structure of S100B bound to the high-affinity target peptide TRTK-12. *J. Mol. Biol. 324*, 1003−1014.
(41) McClintock, K. A., and Shaw, G. S. (2002) Assignment of ^{1}H, ^{13}C and ^{15}N resonances of human Ca^{2+}-S100B in complex with the TRTK-12 peptide. *J. Biomol. NMR 23*, 255−256.
(42) McClintock, K. A., Van Eldik, L. J., and Shaw, G. S. (2002) The C-terminus and linker region of S100B exert dual control on protein-protein interactions with TRTK-12. *Biochemistry 41*, 5421−5428.
(43) McClintock, K. A., and Shaw, G. S. (2003) A novel S100 target conformation is revealed by the solution structure of the Ca^{2+}-S100B-TRTK-12 complex. *J. Biol. Chem. 278*, 6251−6257.
(44) Charpentier, T. H., Thompson, L. E., Liriano, M. A., Varney, K. M., Wilder, P. T., Pozharski, E., Toth, E. A., and Weber, D. J. (2010) The effects of CapZ peptide (TRTK-12) binding to S100B-Ca^{2+} as examined by NMR and X-ray crystallography. *J. Mol. Biol. 396*, 1227−1243.
(45) Garbuglia, M., Verzini, M., Rustandi, R. R., Osterloh, D., Weber, D. J., Gerke, V., and Donato, R. (1999) Role of the C-terminal extension in the interaction of S100A1 with GFAP, tubulin, the S100A1- and S100B-inhibitory peptide, TRTK-12, and a peptide derived from p53, and the S100A1 inhibitory effect on GFAP polymerization. *Biochem. Biophys. Res. Commun. 254*, 36−41.
(46) Ivanenkov, V. V., Dimlich, R. V., and Jamieson, G. A., Jr. (1996) Interaction of S100a0 protein with the actin capping protein, CapZ: Characterization of a putative S100a0 binding site in CapZ α-subunit. *Biochem. Biophys. Res. Commun. 221*, 46−50.
(47) Barber, K. R., McClintock, K. A., Jamieson, G. A., Jr., Dimlich, R. V., and Shaw, G. S. (1999) Specificity and Zn^{2+} enhancement of the S100B binding epitope TRTK-12. *J. Biol. Chem. 274*, 1502−1508.
(48) Gribenko, A., Lopez, M. M., Richardson, J. M., III, and Makhatadze, G. I. (1998) Cloning, overexpression, purification, and spectroscopic characterization of human S100P. *Protein Sci. 7*, 211−215.
(49) Gribenko, A. V., Hopper, J. E., and Makhatadze, G. I. (2001) Molecular characterization and tissue distribution of a novel member of the S100 family of EF-hand proteins. *Biochemistry 40*, 15538−15548.
(50) Wafer, L. N., Streicher, W. W., McCallum, S. A., and Makhatadze, G. I. (2012) Thermodynamic and kinetic analysis of peptides derived from CapZ, NDR, p53, HDM2, and HDM4 binding to human S100B. *Biochemistry 51*, 7189−7201.
(51) Streicher, W. W., Lopez, M. M., and Makhatadze, G. I. (2009) Annexin I and annexin II N-terminal peptides binding to S100 protein family members: Specificity and thermodynamic characterization. *Biochemistry 48*, 2788−2798.
(52) Wilkins, M. R., Gasteiger, E., Bairoch, A., Sanchez, J. C., Williams, K. L., Appel, R. D., and Hochstrasser, D. F. (1999) Protein identification and analysis tools in the ExPASy server. *Methods Mol. Biol. 112*, 531−552.
(53) Lopez, M. M., and Makhatadze, G. I. (2002) Isothermal titration calorimetry. *Methods Mol. Biol. 173*, 121−126.
(54) Gribenko, A. V., Guzman-Casado, M., Lopez, M. M., and Makhatadze, G. I. (2002) Conformational and thermodynamic properties of peptide binding to the human S100P protein. *Protein Sci. 11*, 1367−1375.
(55) Wiseman, T., Williston, S., Brandts, J. F., and Lin, L.-N. (1989) Rapid measurement of binding constants and heats of binding using a new titration calorimeter. *Anal. Biochem. 179*, 131−137.
(56) Sherrod, P. (2005) *Nonlinear Regression Analysis Program, NLREG*, version 6.3, www.nlreg.com, Nashville, TN.

(57) Eftink, M. R., and Ghiron, C. A. (1976) Exposure of tryptophanyl residues in proteins. Quantitative determination by fluorescence quenching studies. *Biochemistry 15*, 672−680.
(58) Makhatadze, G. I., and Privalov, P. L. (1995) Energetics of protein structure. *Adv. Protein Chem. 47*, 307−425.
(59) Eswar, N., Webb, B., Marti-Renom, M. A., Madhusudhan, M. S., Eramian, D., Shen, M. Y., Pieper, U., and Sali, A. (2007) Comparative protein structure modeling using MODELLER. *Current Protocols in Protein Science*, Chapter 2, Unit 2, 9, Wiley, New York.
(60) Wafer, L. N., Streicher, W. W., and Makhatadze, G. I. (2010) Thermodynamics of the Trp-cage miniprotein unfolding in urea. *Proteins 78*, 1376−1381.
(61) Brokx, R. D., Lopez, M. M., Vogel, H. J., and Makhatadze, G. I. (2001) Energetics of target peptide binding by calmodulin reveals different modes of binding. *J. Biol. Chem. 276*, 14083−14091.
(62) Peterman, B. F. (1979) Measurement of the dead time of a fluorescence stopped-flow instrument. *Anal. Biochem. 93*, 442−444.
(63) Rezvanpour, A., and Shaw, G. S. (2009) Unique S100 target protein interactions. *Gen. Physiol. Biophys. 28* (Special No Focus), F39−F46.
(64) Elliott, P. R., Irvine, A. F., Jung, H. S., Tozawa, K., Pastok, M. W., Picone, R., Badyal, S. K., Basran, J., Rudland, P. S., Barraclough, R., Lian, L. Y., Bagshaw, C. R., Kriajevska, M., and Barsukov, I. L. (2012) Asymmetric mode of Ca^{2+}-S100A4 interaction with nonmuscle myosin IIA generates nanomolar affinity required for filament remodeling. *Structure 20*, 654−666.
(65) Ozorowski, G., Milton, S., and Luecke, H. (2013) Structure of a C-terminal AHNAK peptide in a 1:2:2 complex with S100A10 and an acetylated N-terminal peptide of annexin A2. *Acta Crystallogr. D69*, 92−104.
(66) Dempsey, B. R., Rezvanpour, A., Lee, T. W., Barber, K. R., Junop, M. S., and Shaw, G. S. (2012) Structure of an asymmetric ternary protein complex provides insight for membrane interaction. *Structure 20*, 1737−1745.
(67) Rezvanpour, A., Santamaria-Kisiel, L., and Shaw, G. S. (2011) The S100A10-annexin A2 complex provides a novel asymmetric platform for membrane repair. *J. Biol. Chem. 286*, 40174−40183.
(68) van Dieck, J., Brandt, T., Teufel, D. P., Veprintsev, D. B., Joerger, A. C., and Fersht, A. R. (2010) Molecular basis of S100 proteins interacting with the p53 homologs p63 and p73. *Oncogene 29*, 2024−2035.
(69) Kiss, B., Duelli, A., Radnai, L., Kekesi, K. A., Katona, G., and Nyitray, L. (2012) Crystal structure of the S100A4-nonmuscle myosin IIA tail fragment complex reveals an asymmetric target binding mechanism. *Proc. Natl. Acad. Sci. U.S.A. 109*, 6048−6053.
(70) Moore, B. (1965) A soluble protein characteristic of the nervous system. *Biochem. Biophys. Res. Commun. 19*, 739−744.
(71) Wilder, P. T., Lin, J., Bair, C. L., Charpentier, T. H., Yang, D., Liriano, M., Varney, K. M., Lee, A., Oppenheim, A. B., Adhya, S., Carrier, F., and Weber, D. J. (2006) Recognition of the tumor suppressor protein p53 and other protein targets by the calcium-binding protein S100B. *Biochim. Biophys. Acta 1763*, 1284−1297.
(72) Yu, W. H., and Fraser, P. E. (2001) S100β interaction with tau is promoted by zinc and inhibited by hyperphosphorylation in Alzheimer's disease. *J. Neurosci. 21*, 2240−2246.
(73) Sorci, G., Agneletti, A. L., Bianchi, R., and Donato, R. (1998) Association of S100B with intermediate filaments and microtubules in glial cells. *Biochim. Biophys. Acta 1448*, 277−289.
(74) Garbuglia, M., Verzini, M., Sorci, G., Bianchi, R., Giambanco, I., Agneletti, A. L., and Donato, R. (1999) The calcium-modulated proteins, S100A1 and S100B, as potential regulators of the dynamics of type III intermediate filaments. *Braz. J. Med. Biol. Res. 32*, 1177−1185.
(75) Santamaria-Kisiel, L., Rintala-Dempsey, A. C., and Shaw, G. S. (2006) Calcium-dependent and -independent interactions of the S100 protein family. *Biochem. J. 396*, 201−214.
(76) van Dieck, J., Lum, J. K., Teufel, D. P., and Fersht, A. R. (2010) S100 proteins interact with the N-terminal domain of MDM2. *FEBS Lett. 584*, 3269−3274.
(77) Staneva, I., Huang, Y., Liu, Z., and Wallin, S. (2012) Binding of two intrinsically disordered peptides to a multi-specific protein: A combined Monte Carlo and molecular dynamics study. *PLoS Comput. Biol. 8*, e1002682.
(78) Chen, J. (2009) Intrinsically disordered p53 extreme C-terminus binds to S100B($\beta\beta$) through "fly-casting". *J. Am. Chem. Soc. 131*, 2088−2089.
(79) Trizac, E., Levy, Y., and Wolynes, P. G. (2010) Capillarity theory for the fly-casting mechanism. *Proc. Natl. Acad. Sci. U.S.A. 107*, 2746−2750.
(80) Gsponer, J., and Babu, M. M. (2009) The rules of disorder or why disorder rules. *Prog. Biophys. Mol. Biol. 99*, 94−103.
(81) Shoemaker, B. A., Portman, J. J., and Wolynes, P. G. (2000) Speeding molecular recognition by using the folding funnel: The fly-casting mechanism. *Proc. Natl. Acad. Sci. U.S.A. 97*, 8868−8873.
(82) Kiefhaber, T., Bachmann, A., and Jensen, K. S. (2011) Dynamics and mechanisms of coupled protein folding and binding reactions. *Curr. Opin. Struct. Biol. 22*, 21−29.
(83) Zimmer, D. B., Eubanks, J. O., Ramakrishnan, D., and Criscitiello, M. F. (2013) Evolution of the S100 family of calcium sensor proteins. *Cell Calcium 53*, 170−179.
(84) Rety, S., Osterloh, D., Arie, J. P., Tabaries, S., Seeman, J., Russo-Marie, F., Gerke, V., and Lewit-Bentley, A. (2000) Structural basis of the Ca^{2+}-dependent association between S100C (S100A11) and its target, the N-terminal part of annexin I. *Structure 8*, 175−184.
(85) Bhattacharya, S., Large, E., Heizmann, C. W., Hemmings, B., and Chazin, W. J. (2003) Structure of the Ca^{2+}/S100B/NDR kinase peptide complex: Insights into S100 target specificity and activation of the kinase. *Biochemistry 42*, 14416−14426.
(86) Rustandi, R. R., Baldisseri, D. M., Drohat, A. C., and Weber, D. J. (1999) Structural changes in the C-terminus of Ca^{2+}-bound rat S100B($\beta\beta$) upon binding to a peptide derived from the C-terminal regulatory domain of p53. *Protein Sci. 8*, 1743−1751.
(87) Fohr, U. G., Heizmann, C. W., Engelkamp, D., Schafer, B. W., and Cox, J. A. (1995) Purification and cation binding properties of the recombinant human S100 calcium-binding protein A3, an EF-hand motif protein with high affinity for zinc. *J. Biol. Chem. 270*, 21056−21061.
(88) Gingras, A. R., Basran, J., Prescott, A., Kriajevska, M., Bagshaw, C. R., and Barsukov, I. L. (2008) Crystal structure of the Ca^{2+}-form and Ca^{2+}-binding kinetics of metastasis-associated protein, S100A4. *FEBS Lett. 582*, 1651−1656.
(89) Sathe, K., Maetzler, W., Lang, J. D., Mounsey, R. B., Fleckenstein, C., Martin, H. L., Schulte, C., Mustafa, S., Synofzik, M., Vukovic, Z., Itohara, S., Berg, D., and Teismann, P. (2012) S100B is increased in Parkinson's disease and ablation protects against MPTP-induced toxicity through the RAGE and TNF-α pathway. *Brain 135*, 3336−3347.
(90) Schaf, D. V., Tort, A. B., Fricke, D., Schestatsky, P., Portela, L. V., Souza, D. O., and Rieder, C. R. (2005) S100B and NSE serum levels in patients with Parkinson's disease. *Parkinsonism & Related Disorders 11*, 39−43.
(91) Griffin, W. S., Yeralan, O., Sheng, J. G., Boop, F. A., Mrak, R. E., Rovnaghi, C. R., Burnett, B. A., Feoktistova, A., and Van Eldik, L. J. (1995) Overexpression of the neurotrophic cytokine S100β in human temporal lobe epilepsy. *J. Neurochem. 65*, 228−233.
(92) Nonaka, D., Chiriboga, L., and Rubin, B. P. (2008) Differential expression of S100 protein subtypes in malignant melanoma, and benign and malignant peripheral nerve sheath tumors. *J. Cutaneous Pathol. 35*, 1014−1019.
(93) Tarhini, A. A., Stuckert, J., Lee, S., Sander, C., and Kirkwood, J. M. (2009) Prognostic significance of serum S100B protein in high-risk surgically resected melanoma patients participating in Intergroup Trial ECOG 1694. *J. Clin. Oncol. 27*, 38−44.
(94) Camby, I., Nagy, N., Lopes, M. B., Schafer, B. W., Maurage, C. A., Ruchoux, M. M., Murmann, P., Pochet, R., Heizmann, C. W., Brotchi, J., Salmon, I., Kiss, R., and Decaestecker, C. (1999) Supratentorial pilocytic astrocytomas, astrocytomas, anaplastic astro-

cytomas and glioblastomas are characterized by a differential expression of S100 proteins. *Brain Pathol. 9*, 1−19.
(95) Nagy, N., Brenner, C., Markadieu, N., Chaboteaux, C., Camby, I., Schafer, B. W., Pochet, R., Heizmann, C. W., Salmon, I., Kiss, R., and Decaestecker, C. (2001) S100A2, a putative tumor suppressor gene, regulates in vitro squamous cell carcinoma migration. *Lab. Invest. 81*, 599−612.
(96) Bulk, E., Sargin, B., Krug, U., Hascher, A., Jun, Y., Knop, M., Kerkhoff, C., Gerke, V., Liersch, R., Mesters, R. M., Hotfilder, M., Marra, A., Koschmieder, S., Dugas, M., Berdel, W. E., Serve, H., and Muller-Tidow, C. (2009) S100A2 induces metastasis in non-small cell lung cancer. *Clin. Cancer Res. 15*, 22−29.
(97) Suzuki, F., Oridate, N., Homma, A., Nakamaru, Y., Nagahashi, T., Yagi, K., Yamaguchi, S., Furuta, Y., and Fukuda, S. (2005) S100A2 expression as a predictive marker for late cervical metastasis in stage I and II invasive squamous cell carcinoma of the oral cavity. *Oncol. Rep. 14*, 1493−1498.
(98) Deloulme, J. C., Assard, N., Mbele, G. O., Mangin, C., Kuwano, R., and Baudier, J. (2000) S100A6 and S100A11 are specific targets of the calcium- and zinc-binding S100B protein in vivo. *J. Biol. Chem. 275*, 35302−35310.
(99) Fernandez-Fernandez, M. R., Rutherford, T. J., and Fersht, A. R. (2008) Members of the S100 family bind p53 in two distinct ways. *Protein Sci. 17*, 1663−1670.
(100) Hilton, A., Taylor, P., and Walkinshaw, M. D. (2004) Biological Ligands. In *Encyclopedia of Supramolecular Chemistry* (Atwood, J. L., and Steed, J. W., Eds.) Marcel Dekker, New York.
(101) Verdine, G. L., and Hilinski, G. J. (2012) Stapled peptides for intracellular drug targets. *Methods Enzymol. 503*, 3−33.
(102) Kim, Y. W., Kutchukian, P. S., and Verdine, G. L. (2010) Introduction of all-hydrocarbon i,i+3 staples into α-helices via ring-closing olefin metathesis. *Org. Lett. 12*, 3046−3049.
(103) Bernal, F., Wade, M., Godes, M., Davis, T. N., Whitehead, D. G., Kung, A. L., Wahl, G. M., and Walensky, L. D. (2010) A stapled p53 helix overcomes HDMX-mediated suppression of p53. *Cancer Cell 18*, 411−422.
(104) Estieu-Gionnet, K., and Guichard, G. (2011) Stabilized helical peptides: Overview of the technologies and therapeutic promises. *Expert Opin. Drug Discovery 6*, 937−963.
(105) LaBelle, J. L., Katz, S. G., Bird, G. H., Gavathiotis, E., Stewart, M. L., Lawrence, C., Fisher, J. K., Godes, M., Pitter, K., Kung, A. L., and Walensky, L. D. (2012) A stapled BIM peptide overcomes apoptotic resistance in hematologic cancers. *J. Clin. Invest. 122*, 2018−2031.
(106) Sievers, F., Wilm, A., Dineen, D., Gibson, T. J., Karplus, K., Li, W., Lopez, R., McWilliam, H., Remmert, M., Soding, J., Thompson, J. D., and Higgins, D. G. (2011) Fast, scalable generation of high-quality protein multiple sequence alignments using Clustal Omega. *Mol. Syst. Biol. 7*, 539.